

Article

Investigation on Robustness of Model-Based Fuzzy Logic Control Systems

Desislava Stoitseva-Delicheva * and Snejana Yordanova 

Faculty of Automatics, Technical University of Sofia, 1000 Sofia, Bulgaria; sty@tu-sofia.bg

* Correspondence: stoitseva@tu-sofia.bg

Abstract

A novel engineering approach for assessing the robustness of fuzzy logic control (FLC) systems with modified parallel distributed compensation (MPDC) is presented. It addresses the problem of successful implementation and operation in industrial environment of designed systems for the control of complex plants with model uncertainty. The research steps on modified Takagi–Sugeno–Kang (MTSK) plant models MTSK_n and MTSK_{low} already derived and validated for normal and low plant loads from experimental data for the level of the solution in an industrial carbonisation column for soda ash production. MPDC with PI linear local controllers are developed based on the MTSK_n plant model, which differ in the parameters that are optimised by genetic algorithms for fitness functions with and without robustness requirements and different random initial parameter values. The MTSK_n and each of the designed MPDC are represented according to suggested criteria by a nominal and varied linear plant model and controller, respectively. Then, robust stability and robust performance criteria are derived for the linearised MPDC–MTSK_n systems. The system performance and robustness are investigated in the frequency domain and from the simulated reference step responses for MTSK_n and MTSK_{low}, with the results benchmarked against an existing adaptive FLC.

Keywords: level fuzzy logic control; parallel distributed compensation; robust stability; robust performance; simulations; Takagi–Sugeno–Kang plant model

1. Introduction

In the era of increased competition, the intrinsic nonlinearity, model uncertainty and disturbances of contemporary industrial plants demand intelligent techniques for modelling and control to respond to the control system's increased performance requirements. Fuzzy logic controllers (FLCs) become popular in ensuring closed-loop system stability and good performance by simple nonlinear algorithms and design rules based on expert knowledge about the control of the plant. The economical use of computational resources makes them attractive for broad industrial real-time applications via programmable logic controllers.

The most commonly applied FLCs are the model-free Mamdani and Sugeno PID FLCs and the parallel distributed compensation (PDC) built on an existing Takagi–Sugeno–Kang (TSK) plant model. The TSK plant model assumes that the nonlinear plant operates in a small number N of overlapping zones, where the local plant can be described by a linear state-space model. The PDC and the TSK plant model have Sugeno fuzzy units (FUs) that differ only in the conclusions which contain the linear state-space plant models in the TSK plant model and the designed on its basis linear state-space controllers in the



Academic Editor: Yutaka Ishibashi

Received: 9 January 2026

Revised: 4 February 2026

Accepted: 9 February 2026

Published: 11 February 2026

Copyright: © 2026 by the authors.

Licensee MDPI, Basel, Switzerland.

This article is an open access article distributed under the terms and

conditions of the [Creative Commons Attribution \(CC BY\) license](https://creativecommons.org/licenses/by/4.0/).

PDC. The inputs are the measured variables that determine the current operation point. Their membership functions (MFs) outline the expert-defined linearisation zones. The fuzzy inference computes from the premises the degrees μ_i , $i = 1 \div N$ of belonging of the measured inputs to each of the linearisation zones and the degrees of rule activation w_i , which scale the corresponding individual rule conclusion. The FU defuzzified output o is computed as a weighted average of the conclusions qualified (scaled) by w_i of the individual rules.

In ref. [1], a modified TSK plant model (MTSK) and a modified PDC (MPDC) are suggested, where the premise part of the fuzzy rules is separated from the conclusion part. The premise part concludes in a Sugeno FU with a specific rule base that maps the N input MF to N FU outputs $o_j = \mu_j$. The conclusion part contains the parallel-operating local for the linearisation zones linear dynamic plant models or controllers, respectively, which can be described in any form. Most often, the local plant and controller for each zone are conveniently and compactly represented by transfer functions of a comprehensible physical meaning, which are easy for experts to assess. The transfer functions are also the basis of the widely spread engineering approaches for tuning of linear controllers using the well mastered linear control theory.

The main approaches for the design of model-free PID FLC are based on empirical knowledge, linearisation techniques, a linear PID controller, or—complex for engineering use—stability requirements based on linear matrix inequalities, H_∞ , and Popov and Lyapunov criteria [2–9]. The basic part of the PDC design concludes in the design of the local linear control systems accounting for the TSK local plant models and the criteria for stability, desired performance, and robustness. The global PDC system stability is ensured using Lyapunov stability methods and linear matrix inequalities [4,10–12] or frequency-domain approaches [1,13]. The FLC parameters, including the MF and the fuzzy rules, can be optimised most often by genetic algorithms (GAs) and system simulations [14–17]. The TSK model needed is first derived by the linearisation of an existing nonlinear plant model or via GA parameter optimisation of an expert-defined TSK model structure using experimental or simulation data for the plant input and output [1,5,12,15].

The current trend towards vast implementation in industry of fuzzy logic control of various process variables requires enhancement of the FLC and PDC design with simple and easy-to-use engineering techniques for assessment of system robustness, which ensures the feasibility of the designed system and its stable operation in a noisy and changing environment. In [1], robust stability and robust performance criteria are derived for the design of a model-free PID FLC based on the synergism between the criteria for nonlinear system Popov stability and linear system robustness. First, a two-input single-output (2ISO) FLC is transformed into an equivalent single-input single-output (SISO) FLC using the 2ISO FLC control surface projection. Next, the nonlinear plant is represented by an expert-defined nominal linear plant model and plant model uncertainty [18]. Then, the SISO FLC system is turned into Popov's system, to which the Popov stability criterion is applied, accounting for plant model uncertainty [18,19]. The suggested robustness approach is expanded over an adaptive FLC of a PID FLC with an MPDC adaptation of the FLC gains as a function of the plant output [20]. The adaptation of the FLC gains reduces the subjectivity in the FLC expert design and responds to the changes in the plant due to different loads, disturbances, aging, operation modes, etc. Often, the robustness of the FLC system is tested after its design by simulations without considering the impact of the industrial environment [21].

A common drawback of the approaches suggested in the literature for the design of FLC systems is the lack of a simple for use in the engineering practice system robustness

investigation techniques oriented to real plant and disturbance uncertainties in order to guarantee successful system operation in industrial environment.

Hence, the aim of the present research is the development of a novel engineering approach for robustness investigation of an MPDC system illustrated for the control of the level of the solution in an industrial carbonisation column (CCI) for soda ash production. The approach is based on existing MTSK plant models. A novel fitness function with system robustness requirement is suggested for GA optimisation of the local controllers' parameters in the MPDC design. Novel criteria for robust stability and robust performance for a linearised MPDC–MTSK system are derived. The system linearisation is based on representation of the MTSK plant model and the MPDC by nominal linear and worst varied models determined according to suggested criteria from the local linear plant models and controllers, respectively.

The CCI is the installation where soda crystals are produced as a result of a complex exothermic and reversible chemical reaction between the ammonia brine solution fed from the top as inflow, whose level is controlled, and the carbon dioxide gases in a counterflow. Level is a widely distributed variable to be controlled in various industries in order to ensure material and energy balance. It comprises a nonlinear plant subjected to disturbances and plant model uncertainty due to changes in load, modes of operation, operation point, etc. So, FLC appears to be a suitable strategy for its control.

The paper is based on experimental data from the CCI in Solvay Sodi in the town of Devnya, Bulgaria, MATLAB™ (2008b)-Simulink and its toolboxes for fuzzy logic and genetic algorithms [22,23].

The novelty of the present research lies in the approach developed for studying the fitness of a designed MPDC control system for industrial implementation and operation in industrial environment through investigation and improvement of its robustness. The approach is illustrated for the control of an industrial plant, here the solution level in an industrial CCI, which provides necessary realistic data about the plant behaviour. Novel robust stability and robust performance conditions are derived in the frequency domain for the MPDC system. On their basis, the system robustness is investigated and various techniques for its improvement are suggested, such as restarting GA optimisation from different randomly generated initial parameter values in the parameter ranges, which results in different optimal parameters, and a novel robustness-bound fitness function.

The rest of the paper is organised as follows. Section 2 presents the investigation background related to the existing research on linear and adaptive FLC (AFLC) system robustness. Different MPDC are designed in Section 3. The parameters of the MPDC linear PI local controllers are GA-optimised based on a derived MTSK plant model using different initial parameter values and fitness functions. Robust stability and robust performance conditions of an MPDC system are derived in Section 4, representing the MTSK plant model and the MPDC by suggested nominal models and model uncertainty. The robustness and performance of the designed MPDC systems are investigated via simulations and compared with an AFLC system in Section 5. Section 6 includes the conclusion and a vision for future research.

2. Investigation Background

The present investigation on MPDC system robustness is based on Morari–Zafiriou robust stability and robust performance criteria for a linear system that are simple for engineering applications [18]. The plant is assumed to be represented by a family of plant models $F = \{P^o(s), l(s)\}$, defined by expert-assessed nominal plant model $P^o(s)$ and multiplicative model uncertainty $l(s) = \Delta P(s)/P^o(s)$, $\Delta P(s) = P(s) - P^o(s)$, where $P(s)$ is the varied plant model with the worst impact on the closed-loop system stability. The

robust stability criterion requires that the Nyquist plot of the open-loop system, consisting of a linear controller $C(s)$ and a nominal plant model $P^o(s)$, together with the overlaid uncertainty disks for each frequency ω_i from the range D_ω of the significant for the system frequencies, fulfil the Nyquist stability criterion; i.e., the Nyquist plot with the disks is located below and on the right of the Nyquist critical stability point $(-1, j0)$, as illustrated in Figure 1. The uncertainty disk radius r is a function of $l(j\omega)$ and $P^o(j\omega)$. It is computed as the difference between the magnitudes of two vectors:

$$r_i = |P(j\omega_i).C(j\omega_i)| - |P^o(j\omega_i).C(j\omega_i)| = |\Delta P(j\omega_i)| . |C(j\omega_i)| = |l(j\omega_i).P^o(j\omega_i).C(j\omega_i)| \tag{1}$$

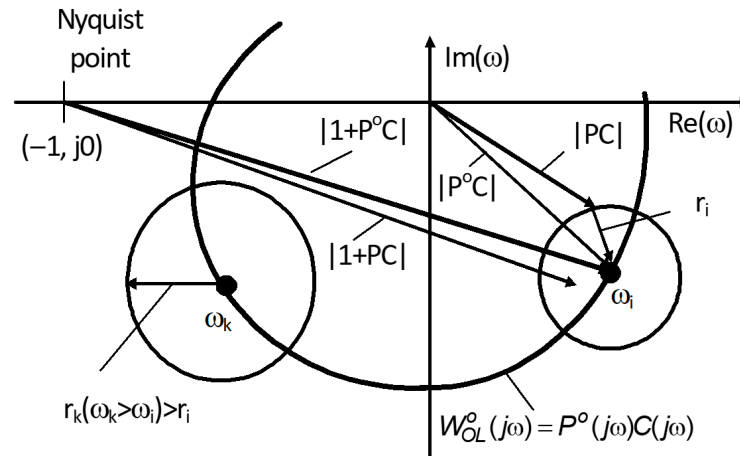


Figure 1. Nyquist plot for plant model's family.

The robust stability condition is satisfied if the magnitude of the vector $|1 + P^o(j\omega).C(j\omega)|$ in Figure 1 is greater than r , $|1 + P^oC| > |l.P^oC|$ for $\forall \omega \in D_\omega$, where $(j\omega)$ is omitted to simplify the expression.

Dividing both sides by $|1 + P^oC|$, the final robust stability criterion takes the following form:

$$|\Phi^o(j\omega).l(j\omega)| < 1 \text{ for } \forall \omega \in D_\omega, \tag{2}$$

where $\Phi^o(j\omega)$ is the frequency response of the closed-loop system with nominal plant model, computed from the closed-loop system transfer function $\Phi^o(s) = P^o(s).C(s).[1 + P^o(s).C(s)]^{-1}$ for $s = j\omega$.

The robust performance criterion is derived as a bounded H_∞ -norm of the error e for all significant frequencies ω and plant models from the family $\mathbf{F} \max_{P \in \mathbf{F}} \sup_{\omega} |e(j\omega)| < 1$, $\forall \omega \in D_\omega$. It is modified to

$$\max_{P \in \mathbf{F}} \sup_{\omega} |S(j\omega).W_f(j\omega)| < 1, \forall \omega \in D_\omega. \tag{3}$$

The substitution applied is based on $e(s) = -S(s)d(s)$, where $S(s) = [1 + P(s).C(s)]^{-1}$ is the closed-loop system sensitivity function and $d(s) = W_f(s).1(s)$ is the disturbance applied at the plant output. The variety of disturbances is described by the shaping filter $W_f(s)$ and its model uncertainty. For most industrial systems, $|W_f(j\omega)| \in [0.3 \div 0.9]$ [18].

Considering the relationship between the sides in a triangle in Figure 1 $|1 + PC| \geq |1 + P^oC| - |l.P^oC|$, their reciprocals $(|1 + PC|)^{-1} \leq (|1 + P^oC| - |l.P^oC|)^{-1}$ and the division by $|1 + P^oC|$ of both the numerator and the denominator of the right-hand expression, it is obtained that $|S| \leq |S^o| (1 - |\Phi^o.l|)^{-1}$. The upper bound is a function of

P^o and l and replaces $|S|$ in (3). Thus, a harder robust performance condition is obtained, $|S^o(j\omega).W_f(j\omega)| (1 - |\Phi^o(j\omega).l(j\omega)|)^{-1} < 1$, or

$$|S^o(j\omega).W_f(j\omega)| + |\Phi^o(j\omega).l(j\omega)| < 1, \forall \omega \in D_\omega. \tag{4}$$

The robust performance criterion (4) contains the robust stability criterion (2), and therefore it is stronger. There is a relationship between the frequency response magnitudes of the sensitivity function $|S(j\omega)|$ and the closed-loop system $|\Phi^o(j\omega)|$. They complement each other to 1, $|S^o(j\omega)| + |\Phi^o(j\omega)| = 1$, $P^o(s).C(s).[1 + P^o(s).C(s)]^{-1} + [1 + P^o(s).C(s)]^{-1} = 1$. Thus, the decreased sensitivity to disturbances causes a corresponding deterioration of the nominal system performance. A way out is a reasonable trade-off between robustness and nominal system performance.

In ref. [20], robust stability and robust performance criteria are derived for a suggested adaptive PID 2ISO FLC (AFLC) system using the example of level control by modification of the Morari–Zafiriou approach. The AFLC consists of a 2ISO PD FLC with a linear integrator of the system error in parallel and an adaptation mechanism based on the MPDC principle. The MPDC is composed of a Sugeno model and local gains K_{aj} and K_{ij} of the PD FLC post-processing and of the integrator, respectively. The Sugeno model has the current measured level H for input and orthogonal MF μ_j , $\sum \mu_j = 1$, which define the linearisation zones that, for the level control, are three, $j = 1 \div 3$. A specific rule base ensures mapping of the MF at the outputs $o_j = \mu_j$, which scale the local for each j -th linearisation zone GA-optimised gains K_{aj} and K_{ij} . The final gains are computed as weighted average of the local gains $K_a = \sum \mu_j.K_{aj}$, $K_i = \sum \mu_j.K_{ij}$ and change with the level since $\mu_j(H)$.

In order to study the AFLC system robustness, the system nonlinear components are linearised. The MPDC of the Sugeno model and the local gains is represented by the families $F_{K_a} = \{K_a^o, \Delta K_a\}$ and $F_{K_i} = \{K_i^o, \Delta K_i\}$. The local gains for linearisation zone “Norm” are commonly accepted for nominal gains K_a^o and K_i^o . The additive uncertainties $\Delta K_a = K_a - K_a^o$ and $\Delta K_i = K_i - K_i^o$ with the varied gains K_a and K_i cover the range of gains adaptation. The complex nonlinear plant is also described by the family $F_P = \{P^o(s), \Delta P(s)\}$, where experts assess the nominal plant model $P^o(s)$ for the most often used operation point and the worst varied plant model $P(s)$ for the heaviest operation conditions.

Then, the nonlinear function $o_{FLC} = \Psi(e, de)$ that describes the 2ISO FU with output o_{FLC} and inputs the system error e and its derivative $de = \dot{e}$ is linearised: $\Psi(e, de) \approx K_1e + K_2de$. Considering that de is computed by a differentiator of the system error with transfer function $W_d(s)$, $de(s) = W_d(s).e(s)$, and accepting the maximal gain $K_1 = K_2 = K = \max$, the transfer function of the linearised 2ISO PD FLC becomes $W_{PD}(s) \approx K.K_a.[1 + W_d(s)]$. In ref. [20], the suggested approach for 2ISO PD FLC linearisation includes a 2ISO FU approximation by an equivalent SISO FU with the signed distance $ds = e + \lambda \dot{e}$ as an input, normalised by the help of K_{ds} in the range $[-1, 1]$ [24]. Then, the sector-bounded control curve of the SISO FU is linearised by the upper sector line with gain K . Accounting for the linearised SISO FU and the pre- and post-processing, the SISO PD FLC transfer function becomes $W_{PD}(s) \approx K.K_{ds}.K_a.[1 + W_d(s)]$.

As a result, the robust stability and robust performance criteria for the linearised SISO equivalent of the 2ISO PID AFLC system can be expressed as (2) and (4) but for different linearised controller and multiplicative uncertainty, which modify all frequency responses in (2) and (3). The linearised controller contains the adaptation gains. Its transfer function for nominal gains is $C_{lin}^o(s) = K.K_{ds}.K_a^o[1 + W_d(s)] + K_i^o/s$ and for varied gains $C_{lin}(s) = K.K_{ds}.(K_a^o + \Delta K_a)[1 + W_d(s)] + (K_i^o + \Delta K_i)/s$. The modified multiplicative uncertainty is $l(s) = [C_{lin}(s)P(s) - C_{lin}^o(s).P^o(s)]/[C_{lin}^o(s).P^o(s)]$. It corresponds to the same uncertainty disks overlaid for different frequencies over the nominal Nyquist plot in Figure 1, which now are determined not only by changes in the plant model but

also by changes in the controller. The new frequency responses in (2) and (4) are computed for $s = j\omega$ from the corresponding transfer functions for the modified uncertainty $l(s)$, the system sensitivity function $S^o(s) = [1 + C_{lin}^o(s).P^o(s)]^{-1}$ and the closed-loop system $\Phi^o(s) = C_{lin}^o(s).P^o(s).[1 + C_{lin}^o(s).P^o(s)]^{-1}$. The superscript 'o' denotes nominal plant model and adaptation gains and the subscript 'lin' a linearised controller.

The satisfaction of the robust stability and robust performance conditions for the linearised SISO FU, the family of plant models that represents the nonlinear plant, and the families that describe the PDC adaptation of the FLC parameters in the expected ranges ensures stability of the initial 2ISO AFLC. The modified robustness criteria (2) and (4) can also be applied in case of adaptation of only one of the gains by accepting zero additive uncertainty for the other gain as well as for AFLC with an SISO FU or various structures and adaptation principles.

The modified criteria (2) and (4) are used to study the robustness of a designed AFLC system for a nominal plant model for the control of the level in an industrial CCI in [16] with adaptation of K_a and K_i . This system is further used in the paper as a benchmark.

3. MPDC System Design and GA Parameter Optimisation

The GA optimisation applied to plant TSK modelling and design of different controllers is based on an algorithm similar to that explained in [25] for tuning of a PI PDC. The main differences are in the experimental data, the simulation model of the closed-loop system with the plant TSK model and the controller, the plan of the simulation experiments, the optimising parameters and their ranges and the fitness function and the extra criterion accepted.

The AFLC has a complex structure that includes two FUs of the 2ISO PD FLC and of the SISO MPDC Sugeno model and an integrator of e in parallel to the PD FLC. Moreover, the computation of the input de of the 2ISO FU is approximate and noise-sensitive, usually using a differentiator of e . The PID AFLC tuning parameters are the MPDC local gains K_{aj} and K_{ij} , which are GA-optimised. The accepted fitness function of the mean squared error (MSE) and the relative control variance is computed from simulations of the closed-loop system with a derived MTSK plant model. The PID AFLC is nonlinear due on the one hand to the 2ISO FU of the PD FLC and the MPDC adaptation of K_a depending on the level. On the other hand, the MPDC adaptation of K_i turns the linear integrator in parallel to the PD FLC into a nonlinear function of the level [20].

In the present research designing a simpler PI MPDC controller using the same Sugeno model from the AFLC MPDC adaptation is suggested [20] to softly blend the control actions of the local PI controllers operating in parallel, $C_j(s) = K_{pj} + K_{ij}/s$. Thus, the MPDC with fixed GA-optimised parameters (K_{pj} K_{ij}) of the local controllers produces a control action that is a nonlinear function of the level. Two fitness functions are employed—the one from the PID AFLC design and its modification by adding to it an extra requirement for improving system robustness.

The block diagram of the system with the suggested PI MPDC for N linearisation zones, $N = 3$ for the control of the level in the CCI, is presented in Figure 2. The MPDC design steps on two MTSK plant models previously derived and validated in [26] using expert knowledge and GA parameter optimisation with experimental data collected during the regular operation of the CCI under two different loads. The MTSK models have identical structures, presented in Figure 2, but different parameters of the local plant transfer functions $P_j(s) = K_j[(T_j s + 1).(T_4 s + 1)]^{-1}$, $j = 1 \div N$, as shown in Table 1.

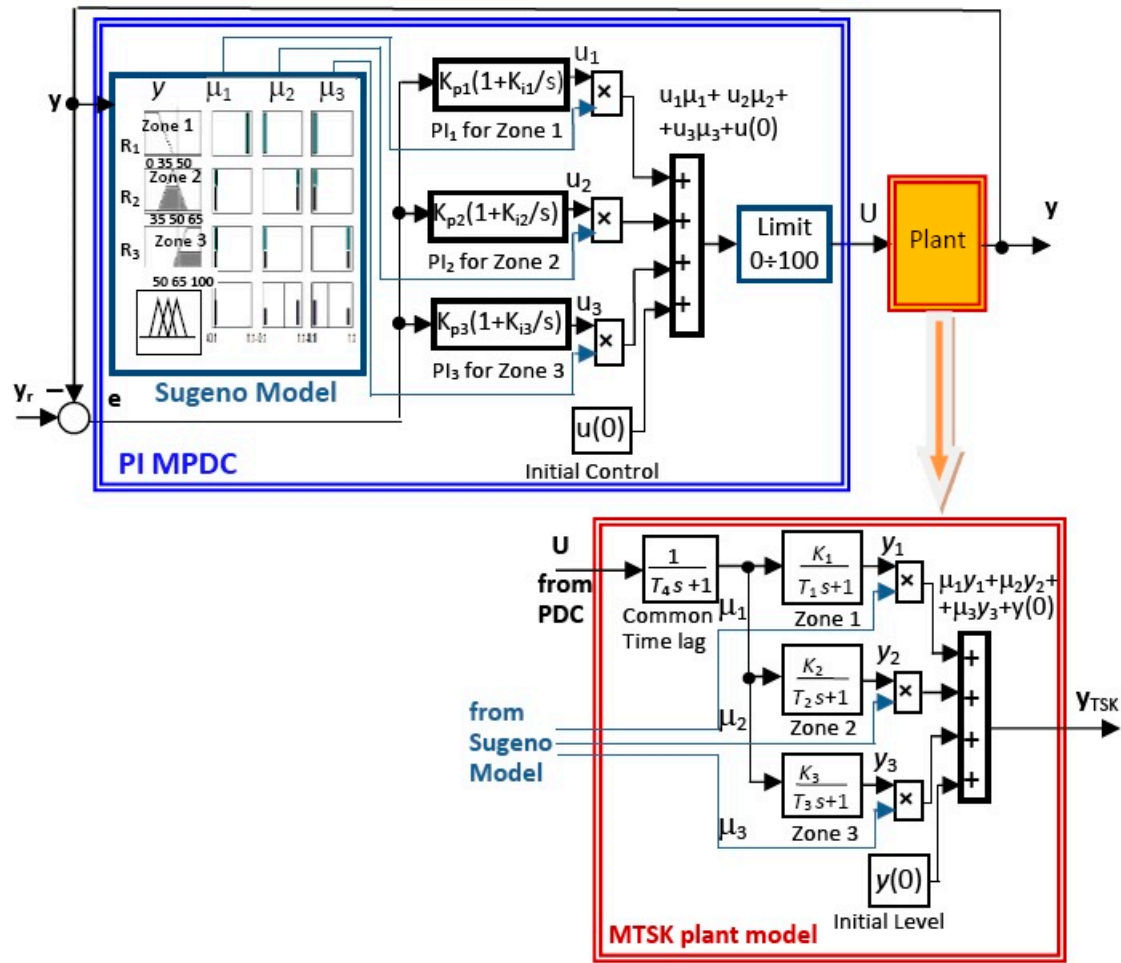


Figure 2. Block diagram of control system MPDC based on MTSK plant model which replaces the plant in simulation.

The Sugeno model of the MTSK plant models is employed in the AFLC MPDC adaptation mechanism and in the suggested MPDC to assess the location of the current operation point in regard to the linearisation zones defined by the MF. The orthogonal MFs for level Low, Norm and High, $MF = [0 \ 0 \ 35 \ 50; 35 \ 50 \ 65; 50, 65 \ 100 \ 100]$, are expert-defined for three linearisation zones around the most often used references 40%, 50% and 60% for the control of the level in the CCI. Its input is the plant output, i.e., the level $y = H$ of the solution in the CCI, which measured value H_k at time t_k determines the current operation point. Specific fuzzy rules with singletons 1 and 0 in the conclusions ensure that the three outputs map the MF $o_i = \mu_i$: **IF** y is Low **THEN** $o_1 = 1, o_2 = 0, o_3 = 0$; **IF** y is Norm **THEN** $o_1 = 0, o_2 = 1, o_3 = 0$; **IF** y is High **THEN** $o_1 = 0, o_2 = 0, o_3 = 1$.

The simulated step responses of the two MTSK models in Figure 3 add new knowledge about the plant. The great difference between them is a measure for the considerable industrial plant model uncertainty provoked by the load changes. Besides, the plant nonlinear character is revealed; i.e., equal plant input step changes $du = 5\%$ cause different plant responses in the different operation points and hence different parameters ($K \ T \ \tau$) of the Ziegler–Nichols (ZN) models, assessed from them via graphical approximation. The MTSK plant model for low load (MTSKlow) is accepted as varied and for normal load (MTSKn) as nominal. The two models are further used in the simulation-based GA optimisation of the MPDC parameters and in the study of the system robustness.

Table 1. Local plant models' parameters.

Zones Parameters	Low Load	Normal Load	
	$T_4 = 164 \text{ s}, y(0) = 29\%$	$T_4 = 150 \text{ s}, y(0) = 33\%$	
Nominal local plant			
1. Low	K_1	0.31	$K^o = 0.11$
	$T_1, \text{ s}$	24	73
	$\tau_1, \text{ s}$	24	$\tau^o = 73$
	$T_{ZN1}, \text{ s}; (\tau_1/T_{ZN1})$	164; 0.15	$T^o = 150; 0.49$
	$FP_1 = K_1 \cdot \tau_1 / T_{ZN1}$	0.047	0.054 = min
2. Norm	K_2	0.75	0.28
	$T_2, \text{ s}$	219	350
	$\tau_2, \text{ s}$	164	150
	$T_{ZN2}, \text{ s}; (\tau_2/T_{ZN2})$	219; 0.75	350; 0.43
	$FP_2 = K_2 \cdot \tau_2 / T_{ZN2}$	0.56	0.12
Varied local plant			
3. High	K_3	1	$K = 0.51$
	$T_3, \text{ s}$	481	98
	$\tau_3, \text{ s}$	164	$\tau = 98$
	$T_{ZN3}, \text{ s}; (\tau_3/T_{ZN3})$	481; 0.34	$T = 150; 0.65$
	$FP_3 = K_3 \cdot \tau_3 / T_{ZN3}$	0.34	0.33 = max

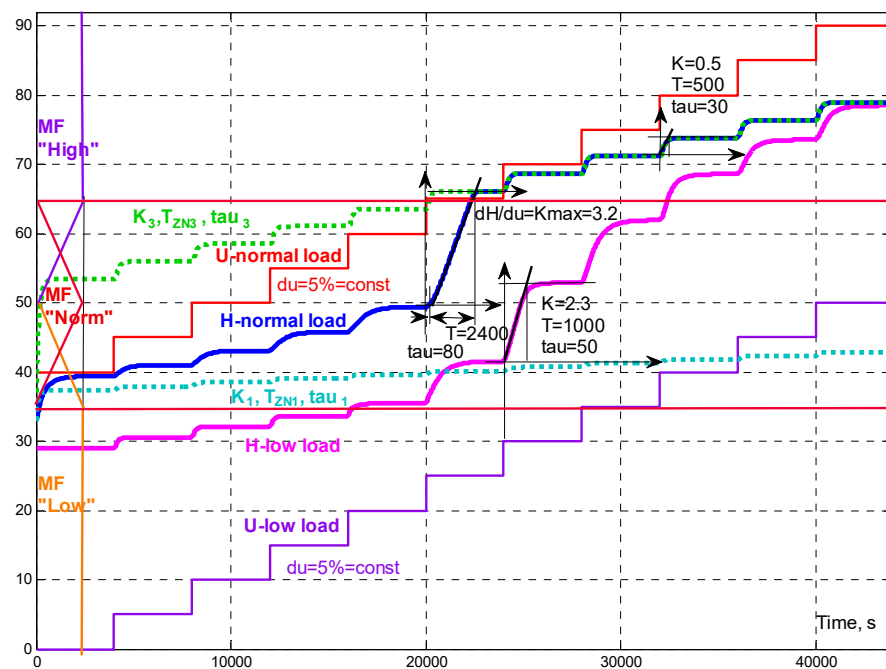


Figure 3. Simulated step responses of the MTSK plant models and the MFs distribution.

The parameters of the local PI controllers (K_{pj}, K_{ij}) are computed for three runs of GA optimisation for each of the two accepted fitness functions:

$$F = \text{MSE} + \theta \cdot D(U/H_r) / D_p \tag{5}$$

$$F_{\text{rob}} = F + \max_k |e_k^o - e_k|. \tag{6}$$

Each new run starts from different randomly generated initial values of the parameters in the ranges around their empirically tuned values and leads to different optimised values of the parameters. The fitness function (5) is used in the parameter optimisation of the AFLC. It integrates the mean squared error for a sample of M values $MSE = \sum_{k=1}^M e_k^2 / M$ and the relative control variance $D(U/H_r)$ with respect to the reference for the level H_r per unit variance D_p of the main disturbance—the pressure P in the solution supply pipe recorded during the real-time operation of the industrial CCl. The minimisation of MSE increases the system dynamic accuracy. The minimisation of $D(U/H_r)/D_p$ smooths the control action, thus reducing the wearing of the final control elements. The scaling factor $\theta = 1.5$ is empirically tuned to balance the contribution of the two components to the criteria. The newly suggested fitness function (6) modifies (5) by including an extra term as a measure for system robustness, the maximal at some time instant t_k absolute difference $\max_k |e^o - e| = \max_k |e_k^o - e_k|$ between the errors e^o and e of the systems with nominal and varied MTSK plant model and MPDC controller. System simulations with the MTSK_n plant model enable the computation of F . The computation of $\max_k |e^o - e|$ from F_{rob} also requires simulations of the system with the varied MTSK_{low} plant model. The GA optimisation in each case ends with reaching $MSE \leq 10.5$ and $\max_k |e^o - e| \leq 9.5$ estimated from system responses to changes of $H_r = 50-60-50-40-50, \%$ with step $\Delta H_r = 10, \%$.

The GA-optimised parameters of the local PI controllers from various initial values for each of the two fitness functions are systemised in Table 2. The accepted end conditions ensure reaching close optimal values of the performance and robustness indicators F_{rob} , MSE, F and $\max_k |e^o - e|$ for different optimised parameters. The GA optimisation based on (6) decreases the optimal value for $\max_k |e^o - e|$. According to Table 2, the PDC1 and PDC1_r systems have the worst performance indicators. Despite the close optimal values for F and F_{rob} and their components, the different optimal MPDC parameters are expected to have a different impact on system robustness. Moreover, the MPDC parameters are optimised for the specific system input and cannot ensure system stability and good performance for different reference changes and industrial disturbances.

Table 2. Local PI controllers’ parameters.

Criterion (Fitness Function)	Variants of MPDC PI Parameters	K_{p1}, T_{i1} K_{p1}/T_{i1} Low	K_{p2}, T_{i2} K_{p2}/T_{i2} Norm	K_{p3}, T_{i3} K_{p3}/T_{i3} High	Nominal (K_p, T_i) ^o and Varied (K_p, T_i) Parameters	$F_{rob}, MSE, F, \max_k e^o - e $
F = min	1 (PDC1)	2.6, 560 0.0047	3.8, 660 0.0058 = max₁	0.8, 676 0.0012 = min₁	(0.8, 676) ^o (3.8, 660)	25.8, 10.5, 16.8, 9
	2 (PDC2)	3.09, 355 0.0087 = max₂	6.18, 750 0.0082	0.92, 641 0.0014 = min₂	(0.92, 641) ^o (3.09, 355)	24.7, 8.6, 15.5, 9.2
	3 (PDC3)	3.68, 541 0.0068 = max₃	5.4, 917 0.0059	0.87, 806 0.0011 = min₃	(0.87, 806) ^o (3.68, 541)	24.6, 8.6, 15.2, 9.4
$F_{rob} = \min$	1 (PDC1 _r)	6, 396 0.015 = max_{1r}	4.3, 454 0.0095	4.1, 644 0.009 = min_{1r}	(4.1, 644) ^o (6, 396)	26, 10.5, 17.9, 8.1
	2 (PDC2 _r)	4.83, 462 0.0105 = max_{2r}	5, 373 0.0134	3.38, 766 0.0044 = min_{2r}	(3.38, 766) ^o (4.83, 462)	23.6, 8.8, 15.7, 7.8
	3 (PDC3 _r)	5.1, 474 0.0108 = max_{3r}	5, 435 0.0115	3.4, 693 0.0049 = min_{3r}	(3.4, 693) ^o (5.1, 474)	23.78, 8.8, 15.8, 8

4. MPDC System Robust Stability and Robust Performance

In order to study the MPDC system robustness, robust stability and robust performance criteria are derived based on a linearisation technique similar to that suggested in [20]. For that purpose, the nonlinear plant is represented by a family of linear

models $F_P = \{P^o(s), l_P(s)\}$, determined by a nominal plant model $P^o(s)$ and the worst multiplicative plant model uncertainty $l_P(s) = \Delta P(s)/P^o(s)$, $\Delta P(s) = P(s) - P^o(s)$, where $P(s)$ is the varied plant model.

Here, it is suggested that the nominal and varied linear plant models are determined from the MTSKn local ZN plant models. A criterion **FP** is accepted to measure which local plant model has the smallest and which has the worst impact on the closed-loop system stability. For local ZN plant models, it can be accepted that $\mathbf{FP} = K \cdot \tau / T$, which reflects that a great gain K and/or a time delay τ and/or a small time constant T of a ZN plant model, each separately and in combination, constitute a great threat to the system stability. Therefore, the MTSKn local ZN plant model with the smallest value $\mathbf{min}_j \mathbf{FP}_j$ of the criterion is accepted for a nominal linear plant model. The worst varied plant model is determined from all other MTSKn local plant models with the greatest value $\mathbf{max}_j \mathbf{FP}_j$ of the criterion.

In the same manner, the nonlinear MPDC with local linear controllers is represented by a family of linear controllers $F_C = \{C^o(s), l_C(s)\}$. The nominal $C^o(s)$ is a local controller with parameters that ensure the smallest threat to system stability according to a suggested criterion \mathbf{FC}_j . In case of PI local controllers, it can be accepted $\mathbf{FC} = K_p \cdot K_i$, $K_i = 1/T_i$. The criterion reflects that the high controller's proportional and integrating gains K_p and K_i , each and both, have the worst impact on the closed-loop system stability. The worst varied controller $C(s)$ is selected from the other local controllers for which $\mathbf{FC}_j = \mathbf{max}_j$. The worst multiplicative controller uncertainty $l_C(s)$ is computed from $l_C(s) = \Delta C(s)/C^o(s)$, $\Delta C(s) = C(s) - C^o(s)$.

The MPDC system robust stability is derived from Figure 1, applying the approaches suggested in [18,20]. The radius of the uncertainty disks around each point of the nominal Nyquist plot $P^o(j\omega) \cdot C^o(j\omega)$ for a given frequency depends on the variations both of the plant model and the controller:

$$r_i = |P(j\omega_i) \cdot C(j\omega_i)| - |P^o(j\omega_i) \cdot C^o(j\omega_i)| = |[P^o(j\omega_i) + \Delta P(j\omega_i)] \cdot [C^o(j\omega_i) + \Delta C(j\omega_i)]| - |P^o(j\omega_i) \cdot C^o(j\omega_i)|. \tag{7}$$

After opening of the brackets, the radius becomes $r = |P^o \cdot C^o| + |\Delta P \cdot C^o + P^o \cdot \Delta C + \Delta P \cdot \Delta C| - |P^o \cdot C^o|$, where $(j\omega)$ is omitted for convenience of writing. Considering that $\Delta P = l_P \cdot P^o$, $\Delta C = l_C \cdot C^o$, r is obtained:

$$r = |l_P \cdot P^o \cdot C^o + l_C \cdot P^o \cdot C^o + l_P \cdot l_C \cdot P^o \cdot C^o| = |P^o \cdot C^o \cdot (l_P + l_C + l_P \cdot l_C)| = |P^o \cdot C^o \cdot l_\Sigma|, \quad l_\Sigma = l_P + l_C + l_P \cdot l_C, \tag{8}$$

where l_Σ is the multiplicative uncertainty due to variations in both the plant model and the controller.

The robust stability criterion requires $|1 + P^o \cdot C^o| > r$ for $\forall \omega \in D_\omega$. Dividing both sides by $|1 + P^o \cdot C^o|$ yields

$$|\Phi^o(j\omega) \cdot l_\Sigma(j\omega)| < 1, \quad \forall \omega \in D_\omega \tag{9}$$

The robust performance criterion is derived based on its general definition (3) from the relationship among the sides of a triangle in Figure 1. $|1 + PC| \geq |1 + P^o C^o| - r$. Considering the reciprocal expressions $(|1 + PC|)^{-1} \leq (|1 + P^o C^o| - r)^{-1}$ and dividing both the numerator and the denominator in the right-hand expression by $|1 + P^o C^o|$, it is obtained $|S| \leq (|1 + P^o C^o|)^{-1} \cdot (|1 - \Phi^o l_\Sigma|)^{-1}$ or $|S| \leq |S^o| \cdot (|1 - \Phi^o l_\Sigma|)^{-1}$. Then the sensitivity function $|S|$ in (3) is substituted by the greater $|S^o| \cdot (|1 - \Phi^o l_\Sigma|)^{-1}$ to yield the stronger condition for robust performance $|S^o W_f| \cdot (|1 - \Phi^o l_\Sigma|)^{-1} < 1$ or finally:

$$|S^o(j\omega) W_f(j\omega)| + |\Phi^o(j\omega) l_\Sigma(j\omega)| < 1, \quad \forall \omega \in D_\omega. \tag{10}$$

The robust stability and robust performance criteria for an MPDC system (9) and (10), respectively, differ from (2) and (4) for a linear system with plant model uncertainty in multiplicative uncertainty. They hold for an MPDC system with defined nominal and

varied plant models and controllers from the available MTSK local plant models and the MPDC local controllers, respectively. The robust stability (9) and robust performance (10) conditions can also be applied to any other control system where both the plant and the controller are subjected to bounded changes. The satisfaction of (9) and (10) ensures that the closed-loop system, designed via GA optimisation of the parameters of the local controllers, maintains stability and desired performance even in the worst transition through the different linearisation zones. The fulfilment of (9) and (10) can be ensured by new GA-optimised parameters of the MTSK local plant models and MPDC local controllers, which determine different nominal and varied plant models and controllers. Each new GA optimisation starts with random initial parameter values and reaches the same end condition for different optimised parameter.

The study of the robustness based on (9) and (10) is illustrated for the MPDC system for the control of the level of the solution in a CCI. The local plant models $P_j(s)$ of the derived MTSK plant models from Figure 2 with parameters in Table 1 are approximated for convenience by ZN models $P_{ZNj}(s) = K_j e^{-\tau_j s} (T_{ZNj} s + 1)^{-1}$ with parameters (K_j, T_{ZNj}, τ_j) , presented in Table 1. The time delay $\tau_j = \min(T_j, T_4)$ and the time constant $T_{ZNj} = \max(T_j, T_4)$, $\tau_j < T_{ZNj}$ are determined considering the approximation of the pure time delay by the linear terms of the Taylor's series expansion $e^{-\tau s} \approx (\tau s + 1)^{-1}$. The selection of ZN models is based on their wide engineering use for describing most of the industrial processes by a small number of parameters with clear physical meaning, which facilitates the formulation of criteria for determination of the nominal and varied plant models from the MTSK local plant models.

The accepted criterion that measures the local plant model impact on the system stability is $FP_j = K_j \cdot \tau_j / T_{ZNj}$. The impact is the worst for the greatest value for FP_j . From Table 1, the nominal linear plant model with the smallest FP_j , $\min_j FP_j$, is $P^o(s) = P_{ZN1}(s)$, where $P_{ZN1}(s)$ is the ZN local plant model of MTSK_n in linearisation zone 'Low' ($j = 1$). The worst varied linear plant model $P(s)$ is the local ZN plant model of MTSK_n in zone 'High' $P(s) = P_{ZN3}(s)$ with parameters $K^o = K_3$, $T^o = T_{ZN3}$, $\tau^o = \tau_3$ with maximal FP_j , $\max_j FP_j$, as seen in Table 1. Thus, the family $F_P = \{P^o(s), l_P(s)\}$ of linear models that represents the nonlinear plant is determined. The step responses of the nominal and varied linear plant models, shown in dotted line in Figure 3, enclose the step responses of the MTSK_n plant model.

The nonlinear MPDC with local linear PI controllers $C_j(s) = K_{pj}(1 + K_{ij}/s)$, $K_{ij} = 1/T_{ij}$ is represented by the family $F_C = \{C^o(s), l_C(s)\}$. The local PI controller that satisfies the accepted criterion $FC_j = \min_j$ is selected as nominal $C^o(s) = K_p^o(1 + K_i^o/s)$, $K_i^o = 1/T_i^o$. The worst varied controller $C(s) = K_p(1 + K_i/s)$, $K_i = 1/T_i$, is determined from the local controllers of the other zones according to the accepted criterion $FC_j = \max_j$. The selected nominal and varied controllers differ for the different optimal parameters of the local PI controllers. The parameters (K_p^o, T_i^o) of the nominal PI controller $C^o(s)$ and (K_p, T_i) of the worst varied PI controller $C(s)$ for all six cases of GA optimisation from three initial values for the tuning parameters for each of the two fitness functions used are presented in Table 2. Different nominal and varied controllers define different worst multiplicative controller uncertainty $l_C(s)$ and family linear models F_C .

5. Investigation of MPDC System Robustness and Analysis of Results

The investigation of the MPDC system aims to identify the impact of various factors on system robustness and performance to help achieve an optimal balance between the two. System robustness is evaluated by the robust stability (9) and robust performance (10) criteria in the frequency domain and by the deviation of the performance indicators of the

system assessed from the simulated step responses with the varied MTSKlow plant model from those of the system with the MTSKn plant model in the time domain.

In Figure 4 are presented the robust stability via dotted lines and robust performance via solid line curves of the MPDC systems with local PI controllers PDC1 ÷ PDC3 and PDC1r ÷ PDC3r from Table 2, computed from the left-hand side of (9) and (10) for $\omega \in D_\omega$. Each curve in solid and dotted lines is labelled in the colour of the curve. The significant frequencies for all systems belong to the estimated range $D_\omega \approx [(10^{-2} \div 1)]\omega_o$, where $\omega_o = 2\pi/T^o$ is the plant natural frequency. The robustness criteria for each system are satisfied for $\omega \in D_{\omega_{rob}}$, $D_{\omega_{rob}} \subseteq D_\omega$, where the corresponding curves are below the border line $1(\omega)$. The derived robust stability and robust performance curves for AFLC in [20] are also added to Figure 4 for comparison. They are computed for the GA-optimised in [16] MPDC local adaptation gains $K_{aj} = [51 \ 32 \ 89]$ and $K_{ij} = [1/34 \ 1/374 \ 1/179]$ that minimise F from (5) and the accepted nominal and varied gains. The nominal and varied linear plant models are the suggested here from the MTSKn local ZN plant model.

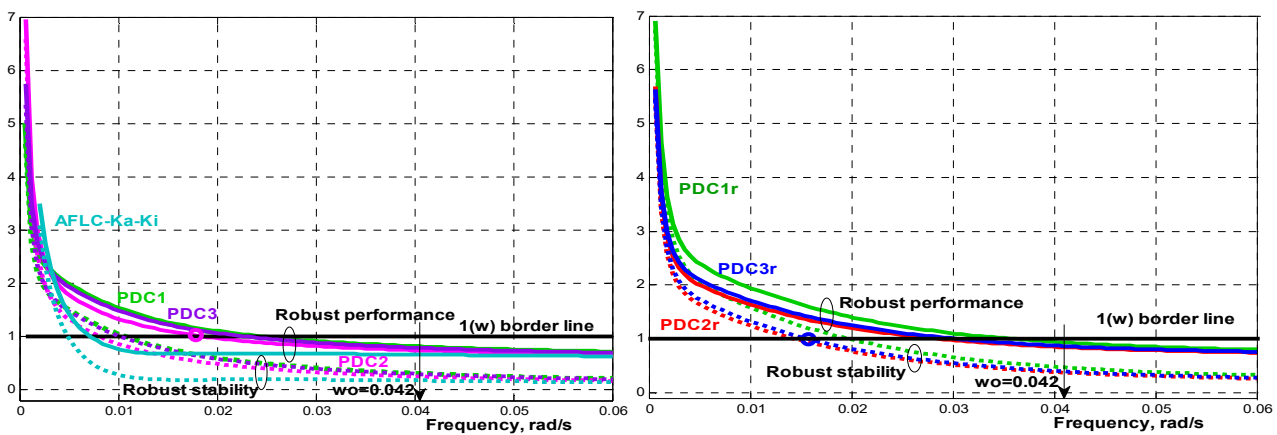


Figure 4. Robust stability and robust performance curves of investigated MPDC and AFLC systems.

The magnitudes of the MPDC multiplicative system uncertainties $|l_\Sigma(j\omega)|$ in solid lines and the magnitude frequency responses of the nominal linear closed-loop systems $|\Phi^o(j\omega)|$ in dotted lines are presented in Figure 5, labelled in the colours of the curves. The different optimised parameters of the local PI controllers for each run of the GA optimisation and the suggested criteria for selection of the nominal and varied controllers on their basis result in different $|l_\Sigma(j\omega)|$ and $|\Phi^o(j\omega)|$ curves for the PDC1 ÷ PDC3 and PDC1r ÷ PDC3r systems, shown in Figure 5. The $|l_\Sigma(j\omega)|$ curves of the PDC1 ÷ PDC3 systems are with 2.5 greater magnitudes than of the curves of the PDC1r ÷ PDC3r systems. The $|l_\Sigma(j\omega)|$ curves of PDC1r ÷ PDC3r systems are close to each other since the nominal plant models and controllers are closed to their varied counterparts. The satisfaction of the robust stability criterion (9) for great values of $|l_\Sigma(j\omega)|$ requires small values of $|\Phi^o(j\omega)|$.

The magnitude frequency responses of the nominal closed-loop systems in Figure 5 enable the assessment of the nominal linear system cutting frequencies ω_c for which $|\Phi^o(j\omega_c)|$ becomes small enough to practically filter the input signals with frequencies greater than ω_c . Here, it is accepted that $|\Phi^o(j\omega_c)| \leq 5\% \cdot |\Phi^o(j0)|$, where $|\Phi^o(j0)| = 1$ corresponds to $y(\infty) = y_r(\infty)$, i.e., steady state in the time domain. The first frequency ω_1 for which the robustness criteria are satisfied in Figure 4 and the cutting frequencies ω_c from the magnitude frequency responses of the nominal closed-loop linear systems in Figure 5 define the range $D_{\omega_{rob}} = [\omega_1, \omega_c]$, $\omega_c > \omega_1$, in which the robustness criteria are practically fulfilled. The small values of $|\Phi^o(j\omega)|$ for great values of $|l_\Sigma(j\omega)|$ determine a low cutting frequency ω_c . A great range $D_{\omega_{rob}}$ determines high system robustness to input signals and plant parameter changes of varying magnitude and frequency.

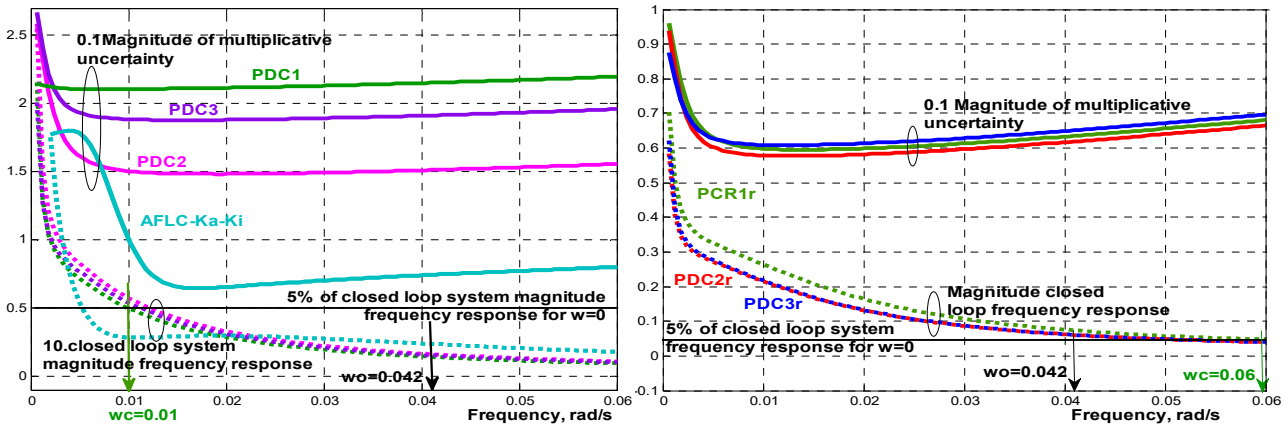


Figure 5. Magnitudes of multiplicative uncertainties and magnitude frequency responses of closed-loop AFLC and MPDC.

The investigation results presented in Figures 4 and 5 answer the questions regarding how system robustness can be improved by different initial values for GA optimisation parameters and by introduction of a robustness-related term in the fitness function. The second factor has a greater impact on the system robustness through the significant change in the range $\omega_c - \omega_1$.

The simulated MPDC systems' reference step responses of level and control action are displayed in Figures 6 and 7. The references are the most often used for the level in the CCI and change in the sequence $H_r = 50-60-50-40-50$, % to enable assessing the nonlinear system performance in different operating points, i.e., linearisation zones where the local plant models and controllers are different. The fulfilment of the robustness criteria (9) and (10) ensures close system performance indicators in the different zones, i.e., system robustness in the transition from one to another linearisation zone. The first transient response for fixed $H_r = 50$, % is for establishing equilibrium initial conditions. In Figure 8, the step responses of level and control action of the PDC3 and PDCr3 systems selected as the best are compared with those of the AFLC system. All step responses are simulated for systems with nominal and varied MTSKlow plant models derived for low CCI load. Thus, the system robustness to changes in the characteristics of the nonlinear plant in each zone can be assessed. Figures 6–8 show the importance of the inclusion of a robustness term in the fitness function in the GA optimisation of the MPDC parameters since it improves system robustness at the expense of a nominal system with decreased dynamic accuracy and increased control action span. This inclusion increases the range $\omega_c - \omega_1$, assessed from the robustness curves, thus relating the frequency-domain and time-domain measures for system robustness. The frequency-domain robustness criteria are more general as they show the frequency range of input signals for which robustness is ensured.

The relationship between the performance and the robustness of the systems designed for various fitness functions and initial values in the GA parameter optimisation is estimated with respect to the following measures for performance and robustness of MPDC closed-loop systems:

- the mean overshoot from all step responses σ^o_{mean} , $\sigma^o = [(y_r - y) / \Delta y_r] \cdot 100$, %, and the range of settling time t^o_{sr} , s as measures for the system dynamic accuracy;
- the mean span of the control action from all step responses $U^o_{smean} = |U^o_{max} - U^o_{min}|_{mean}$ as a measure for control smoothness;
- the width of the frequency range $D_{\omega_{rob}} = [\omega_1, \omega_c]$, assessed by the difference $\omega_c - \omega_1$, where ω_1 is the first frequency ω^s_1 for which (9) is satisfied and the first frequency ω^p_1 for which (10) is satisfied;

- the absolute difference between the mean overshoots $\Delta\sigma_{\text{mean}} = |\sigma^{\text{o}}_{\text{mean}} - \sigma_{\text{mean}}|, \%$, and settling times $\Delta t_{\text{smax}} = |t^{\text{o}}_{\text{smax}} - t_{\text{smax}}|, \text{s}$ of the systems with nominal and varied MTSK plant models;
- the maximal absolute difference from all step responses between the plant output of the systems with nominal y^{o} and varied y MTSK plant models $\Delta y_{\text{max}} = |y^{\text{o}} - y|_{\text{max}}$;
- the absolute difference between the mean spans of the control action $\Delta U_{\text{smean}} = |U^{\text{o}}_{\text{smean}} - U_{\text{smean}}|, \%$ of the systems with nominal and varied MTSK plant models.

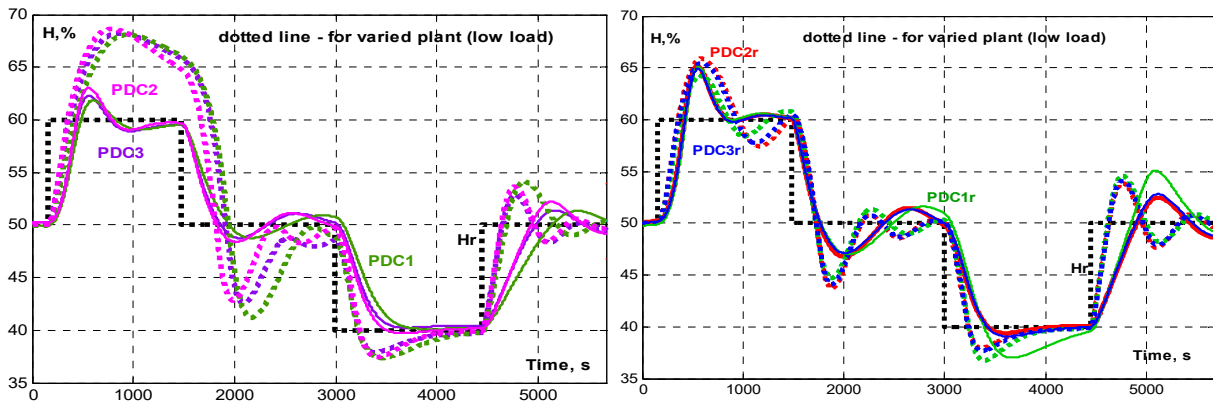


Figure 6. Reference step responses of level of MPDC systems designed for $F = \text{min}$ (left) and $F_{\text{rob}} = \text{min}$ (right).

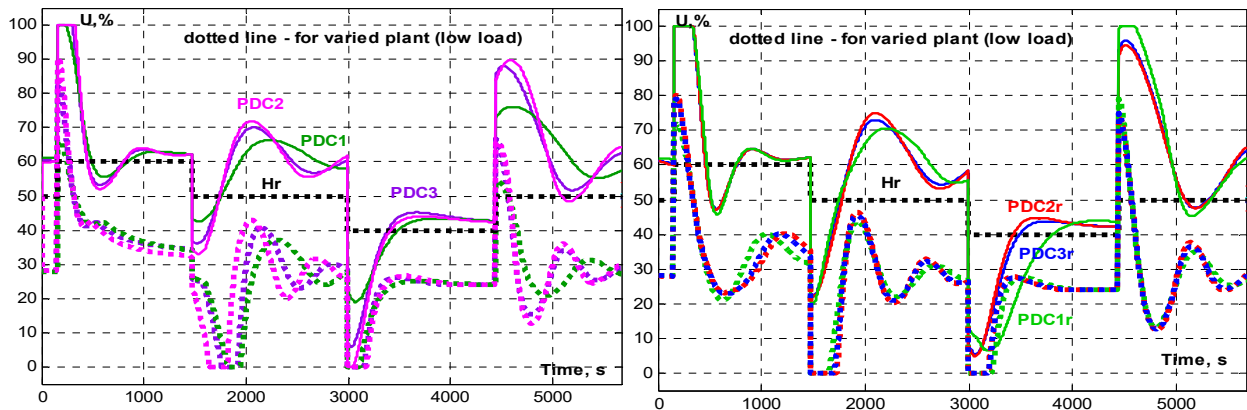


Figure 7. Reference step responses of control action of MPDC systems designed for $F = \text{min}$ (left) and $F_{\text{rob}} = \text{min}$ (right).

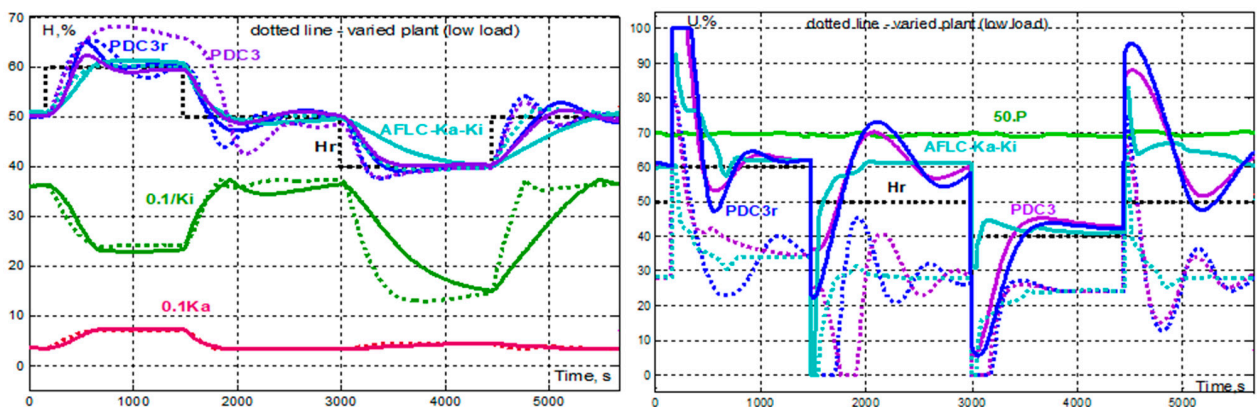


Figure 8. Reference step responses of level (left) and control action (right) of MPDC systems PDC3, PDCr3 and AFLC.

The indicators for systems' dynamic accuracy, control smoothness and robustness are assessed from the corresponding graphs in Figures 4 and 6–8 and systemised in Table 3, where the best values are in bold and the worst are highlighted in grey. The negative width of $D_{\omega_{rob}}$ shows that no robustness criteria are fulfilled in the frequency range that is significant for the system before the cutting frequency.

Table 3. MPDC and AFLC system performance and robustness indicators.

Performance and Robustness Indicators	AFLC System	PDC1 System	PDC2 System	PDC3 System	PDC1r System	PDC2r System	PDC3r System
$\sigma^o_{mean}, \%$	6	11	17	13	40	30	30
t^o_{sr}, s	1500 – 1500	800 ÷ 2000	1000 ÷ 2000	900 ÷ 1900	1000 ÷ 3000	1000 ÷ 2500	1000 ÷ 2500
$U^o_{smean}, \%$	33	33	48	43	48	47	47
$(\omega_c - \omega^s_1)$	(0.001)	(0.001)	(0.006)	(0.002)	(0.04)	(0.038)	(0.037)
$(\omega_c - \omega^p_1)$	(-0.002)	(-0.013)	(-0.01)	(-0.007)	(0.026)	(0.028)	(0.028)
$\Delta\sigma_{mean}, \%$	2	46	38	30	7	10	7
$\Delta t_{smax}, s$	800	∞	∞	∞	1000	1000	1000
$\Delta y_{max}, \%$	6	8	9	8.5	7	5	5
$\Delta U_{smean}, \%$	2	2	7	6	2	2	2
'+'/'-' (sum)	+6/-2 (+4)	+4/-4 (0)	+0/-4 (-4)	+2/-2 (0)	+4/-3 (+1)	+4/0 (+4)	+5/0 (+5)

∞ —does not settle within 1500 s.

The analysis of the graphs leads to the following conclusions:

The impact of the changes in the plant due to the different load on the system performance, assessed by $\Delta\sigma_{mean}$, Δt_{smax} , Δy_{max} and ΔU_{smean} , is reduced when the frequency range $D_{\omega_{rob}}$, for which the robustness criteria are satisfied covers a greater part of the range D_{ω} of significant frequencies for the MPDC system. The degree of overlapping of $D_{\omega_{rob}}$ and D_{ω} is measured by $\omega_c - \omega_1$ as it depends on the frequency ω_1 , when the robustness criteria are first satisfied, and the MPDC system cutting frequency, estimated from the cutting frequency ω_c of the nominal linear closed-loop system.

The PDC1r ÷ PDC3r systems, designed for $F_{rob} = \min$, show the following advantages and drawbacks over the PDC1 ÷ PDC3 systems, designed for $F = \min$:

- a wider frequency range with satisfied robustness criteria;
- better robustness expressed in smaller $\Delta\sigma_{mean}$, Δt_{smax} , Δy_{max} and ΔU_{smean} , assessed from the step responses for nominal and varied MTSK plant models;
- worse performance of the systems with an MTSKn plant model, expressed in higher σ^o_{mean} , t^o_{sr} and U^o_{smean} ;
- close step responses both for nominal and varied MTSK plant models, i.e., insensitive to different initial parameter values in the GA optimisation;
- an insignificant change with load of the system step responses simulated with the varied MTSKlow plant model from the nominal step responses with an MTSKn plant model;
- close control actions for nominal and varied MTSKlow plant models;
- identical greater mean control spans U^o_{smean} and identical smaller changes ΔU_{smean} , i.e., insensitive to different initial parameter values in the GA optimisation.

The PDC1–PDC3 systems and the AFLC system have a narrow frequency range $D^s_{\omega_{rob}}$ with respect to robust stability and negative range $D^p_{\omega_{rob}}$ with respect to robust performance. So, the robust performance criterion (10) is not fulfilled in the frequency

range that is significant for the system, i.e., $\omega_1 > \omega_c$. This is provoked by the high system sensitivity $|S^o(j\omega)|$ to disturbances and changes in the plant characteristics in (10), which determines small values of $|\Phi^o(j\omega)|$ for $\omega \in D_\omega$ and hence small ω_c . The violation of (10) causes deterioration in the system performance. It is felt in the great deviation of the PDC1–PDC3 systems' step responses for a varied MTSKlow plant model from those of the systems with an MTSKn plant model in Figure 6. The impact of the plant changes on the AFLC system step responses for an MTSKn plant model is small, measured by the smallest from all systems $\Delta\sigma_{\text{mean}}$, Δt_{smax} and ΔU_{smean} , as seen in Figure 8. The trade-off with the system dynamic accuracy for an MTSKn plant model is relatively small as σ_{mean}^o , t_{sr}^o and U_{smean}^o are the smallest from all MPDC systems. The control action settles the fastest. This is explained with the adaptation of K_a and K_i , seen in Figure 8, and compensated by the more complex controller's structure and design.

The numbers of the best denoted with '+' and the worst denoted with '-' values of the performance indicators of the investigated systems are presented in Table 3. System PDC3 can be considered the best among the systems designed for $F = \min$ with the greatest sum (+2 – 2 = 0), with equal numbers of advantages and drawbacks. System PDC3r is the best among the systems designed for $F_{\text{rob}} = \min$ and better than PDC3 system with a sum of (+5 – 0 = +5), with 5 more advantages than drawbacks. The step responses for level and control action of the best PDC3 and PDC3r systems are presented in Figure 8 to be compared against the step responses of the AFLC system.

The conclusion is that the PDC3r system is competitive with the AFLC system with respect to robustness and MPDC–MTSKn system performance but has a simpler structure and design. This is due to the inclusion of a requirement for robustness in the fitness function used by the GA optimisation of the PDCr parameters. The criteria for determining the nominal and varied linear plant model and controller also help to satisfy (9) and (10) in a wide frequency range. However, the high robustness of the PDC3r system is achieved at the expense of reduced MPDC–MTSKn system dynamic accuracy.

6. Conclusions

The main contributions of the present research include the following:

A novel engineering approach for the robustness investigation of an MPDC system is developed. It is illustrated for the control of the level of the solution in an industrial carbonisation column for soda ash production. The approach is based on existing MTSK plant models derived and validated from experimental data for normal and low load during the operation of the CCl.

MPDC with local PI controllers is designed. A novel fitness function with a system robustness requirement is suggested for GA optimisation of the local controllers' parameters. The impact of random initial values of the parameters in the GA optimisation on system robustness is studied.

Novel frequency-domain criteria for robust stability and robust performance are derived based on MPDC–MTSK system linearisation, representing the MTSK plant model and the MPDC by linear nominal and worst varied models determined according to suggested criteria from the local linear plant models and controllers, respectively.

The performance and the robustness of the designed MPDC–MTSK systems are studied in the frequency domain and by the time-domain indicators assessed from the simulated step responses of the systems with the MTSK plant model for normal (nominal) and the MTSK plant model for low load (varied). The results show the effectiveness of the novel robustness-bound fitness function and the competitiveness of the simple in structure and design PI MPDC to the existing PID AFLC.

Author Contributions: Conceptualisation, S.Y. and D.S.-D.; methodology, S.Y. and D.S.-D.; software, S.Y.; validation, S.Y. and D.S.-D.; formal analysis, D.S.-D.; investigation, S.Y.; resources, D.S.-D.; data curation, S.Y. and D.S.-D.; writing—original draft preparation, S.Y.; writing—review and editing, D.S.-D.; visualisation, S.Y. and D.S.-D.; supervision, S.Y.; project administration, NA; funding acquisition, NA. All authors have read and agreed to the published version of the manuscript.

Funding: This work has been accomplished with financial support by the European Regional Development Fund within the Operational Programme “Bulgarian national recovery and resilience plan”, procedure for direct provision of grants “Establishing of a network of research higher education institutions in Bulgaria”, and under Project BG-RRP-2.004-0005 “Improving the research capacity and quality to achieve international recognition and resilience of TU-Sofia (IDEAS)”.

Institutional Review Board Statement: Not applicable.

Informed Consent Statement: Not applicable.

Data Availability Statement: Unable to obtain data due to privacy restrictions.

Acknowledgments: This work has been accomplished with financial support by the European Regional Development Fund within the Operational Programme “Bulgarian national recovery and resilience plan”, procedure for direct provision of grants “Establishing of a network of research higher education institutions in Bulgaria”, and under Project BG-RRP-2.004-0005 “Improving the research capacity and quality to achieve international recognition and resilience of TU-Sofia (IDEAS)”.

Conflicts of Interest: The authors declare no conflicts of interest.

Abbreviations

The following abbreviations are used in this manuscript:

CCI	carbonisation column
(A)FL(C)	(adaptive) fuzzy logic (control/ler)
FU	fuzzy unit
GA	genetic algorithm
MF	membership function
MSE	mean squared error
(M)PDC(r)	(modified) parallel distributed compensation (robust)
SISO, 2ISO	single-input single-output, two-input single-output
(M)TSK(n/low)	(modified) Takagi–Sugeno–Kang model (for normal or low load)
ZN	Ziegler–Nichols model

References

1. Yordanova, S. *Methods for Design of Fuzzy Logic Controllers for Robust Process Control*; KING: Sofia, Bulgaria, 2011; ISBN 987-954-9518-68-9. (In Bulgarian)
2. Chao, C.-T.; Sutarna, N.; Chiou, J.-S.; Wang, C.-J. An optimal fuzzy PID controller design based on conventional PID control and nonlinear factors. *Appl. Sci.* **2019**, *9*, 1224. [[CrossRef](#)]
3. Datta, R.; Dey, R.; Bhattacharya, B. Further improved stability condition for T-S fuzzy time-varying delay systems via generalised inequality. *Int. J. Adv. Intell. Paradig.* **2019**, *14*, 310–327. [[CrossRef](#)]
4. Ganesh, E.N.; Bettyjane, J. Simulation and synthesis of TS fuzzy system using parallel distribution compensation technique. *Int. J. Inf. Technol.* **2020**, *12*, 1443–1449. [[CrossRef](#)]
5. Jantzen, J. *Foundations of Fuzzy Control. A Practical Approach*, 2nd ed.; John Wiley and Sons: Chichester, UK, 2013.
6. Venkataraman, A. Design and implementation of adaptive PID and adaptive fuzzy controllers for a level process station. *Adv. Technol. Innov.* **2021**, *6*, 90–105. [[CrossRef](#)]
7. Song, R.; Huang, S.; Xiong, L.; Zhou, Y.; Li, T.; Tan, P.; Sun, Z. Takagi–Sugeno Fuzzy Parallel Distributed Compensation Control for Low-Frequency Oscillation Suppression in Wind Energy-Penetrated Power Systems. *Electronics* **2024**, *13*, 3795. [[CrossRef](#)]
8. Enemegio, R.; Jurado, F.; Villanueva-Tavira, J. Experimental Evaluation of a Takagi–Sugeno Fuzzy Controller for an EV3 Ballbot System. *Appl. Sci. Adv. Electron. Digit. Signal Process.* **2024**, *14*, 4103. [[CrossRef](#)]
9. Rajabpour, L.; Selamat, H.; Barzegar, A.; Fadzli Haniff, M. Design of a robust active fuzzy parallel distributed compensation anti-vibration controller for a hand-glove system. *PeerJ Comput. Sci.* **2021**, *7*, e756. [[CrossRef](#)] [[PubMed](#)]

10. Feng, G. *Analysis and Synthesis of Fuzzy Control Systems: A Model Based Approach*; Taylor & Francis: Abingdon, UK; CRC Press: Boca Raton, FL, USA, 2017.
11. Khan, M.; Siddiqui, A.S.; Mahmoud, A.S.A. Robust H_∞ control of magnetic levitation system based on parallel distributed compensator. *SHAMS Eng. J.* **2018**, *9*, 1119–1129. [[CrossRef](#)]
12. Tanaka, K.; Wang, H. *Fuzzy Control Systems Design and Analysis: A Linear Matrix Inequality Approach*; John Wiley and Sons: New York, NY, USA, 2001.
13. Lan, L.H.; Van Tiem, N.; Van, C.N. Absolute stability for a class of Takagi-Sugeno fuzzy control systems. In Proceedings of the 3rd International Conference on Robotics, Control and Automation Engineering (RCAE 2020), Chongqing, China, 5 October 2020; pp. 47–51.
14. Civelek, Z. Optimization of fuzzy logic (Takagi-Sugeno) blade pitch angle controller in wind turbines by genetic algorithm. *Eng. Sci. Techn. Int. J.* **2020**, *23*, 1–9. [[CrossRef](#)]
15. Ángeles-Hurtado, L.A. Fuzzy Logic and Genetic-Based Algorithm for a Servo Control System. *Micromachines* **2022**, *13*, 586. [[CrossRef](#)] [[PubMed](#)]
16. Rodríguez-Abreo, O.; Rodríguez-Reséndiz, J.; García-Cerezo, A.; García-Martínez, J.R. Fuzzy logic controller for UAV with gains optimized via genetic algorithm. *Heliyon* **2024**, *10*, e26363. [[CrossRef](#)]
17. Sowmya, P.; Balasubram, G.; Rakeshkuma, S.; Ramkumar, K. A Genetic Algorithm Tuned Fuzzy Controller for a Nonlinear Process. *J. Appl. Sci.* **2014**, *14*, 1576–1581. [[CrossRef](#)]
18. Morari, M.; Zafiriou, B. *Robust Process Control*; Prentice Hall: Englewood Cliffs, NJ, USA, 1989; ISBN 0-13-782153-0.
19. Kodkin, V.; Anikin, A.; Kuznetsova, E. Efficiency of Applying the Nyquist and V.M. Popov Criteria for Stability Analysis of Linearized Automatic Control Systems in Electromechanics and Power Engineering. *Energies* **2023**, *16*, 872. [[CrossRef](#)]
20. Yordanova, S.; Slavov, M. Stability analysis of model-free adaptive fuzzy logic control system applied for liquid level control in soda production. *Jordan J. Electr. Eng.* **2023**, *9*, 14–30. [[CrossRef](#)]
21. Bahadori, A.; Ahmadzadeh, M.; Fazeli, R. Design and simulation of a fuzzy logic controller for STATCOM in power systems. *Intell. Model. Electromechanical Syst.* **2025**. [[CrossRef](#)]
22. Fuzzy Logic. *Toolbox: User's Guide for Use with MATLAB*; The MathWorks Inc.: Natick, MA, USA, 1998.
23. MATLAB. *Genetic Algorithm and direct Search Toolbox. User's Guide*; The MathWorks Inc.: Natick, MA, USA, 2004.
24. Choi, B.; Kwak, S.; Kim, B. Design and stability of single-input fuzzy logic controller. *IEEE Trans. Syst. Man Cybern.* **2000**, *30*, 303–309. [[CrossRef](#)] [[PubMed](#)]
25. Yordanova, S.; Slavov, M.; Gueorguiev, B. Optimisation of parallel distributed compensation for real time control of level in carbonisation column. *Autom. Control Comput. Sci.* **2020**, *54*, 379–390. [[CrossRef](#)]
26. Yordanova, S.; Slavov, M.; Stoitseva-Delicheva, D. Load-bound fuzzy logic control of an industrial nonlinear plant. In Proceedings of the 2023 International Scientific Conference on Computer Science (COMSCI), Sozopol, Bulgaria, 18–20 September 2023; pp. 1–9.

Disclaimer/Publisher's Note: The statements, opinions and data contained in all publications are solely those of the individual author(s) and contributor(s) and not of MDPI and/or the editor(s). MDPI and/or the editor(s) disclaim responsibility for any injury to people or property resulting from any ideas, methods, instructions or products referred to in the content.